Evidence of universality in the dynamical response of nanomechanical ultra-nanocrystalline diamond resonators at millikelvin temperatures

Matthias Imboden, Pritiraj Mohanty
Department of Physics, Boston University, 590 Commonwealth Avenue, Boston, Massachusetts 02215, USA
(Dated: January 29, 2009)

We report millikelvin-temperature measurements of dissipation and frequency shift in megahertz-range resonators fabricated from ultra-nanocrystalline diamond. Frequency shift $\delta f/f_0$ and dissipation Q^{-1} demonstrate temperature dependence in the millikelvin range similar to the glass model of two level systems. The logarithmic temperature dependence of $\delta f/f_0$ is in good agreement with the glass model, where phonon relaxation and phonon resonant absorption is observed. Dissipation shows a weak power law, $Q^{-1} \propto T^{\frac{1}{3}}$, followed by saturation at low temperature. A comparison of both the frequency shift and dissipation in equivalent nanomechanical structures made of single-crystal silicon and gallium arsenide indicates universality in the dynamical response.

PACS numbers: 85.85.+j,62.25.-g,65.40.De,81.05.Uw

Nanomechanical resonators are instrumental in the investigation of a wide variety of fundamental physics problems. These include quantum measurement and quantum computation [1, 2], ultra-sensitive force and mass detection [3], single spin detection [4], gravitational wave detection [2] and other fundamental phenomena [5, 6]. The fundamental characteristics of a resonator are determined by the resonance frequency shift δf and dissipation (inverse quality factor) Q^{-1}. In particular, better device response time is obtained by high frequency and low dissipation or loss. Reduced dimensions are necessary for achieving high resonance frequencies. However, miniaturization beyond the sub-micron scale leads to increase in the surface-to-volume ratio, resulting in increased dissipation which limits device performance. To counter this trend it is therefore necessary to avoid extrinsic mechanisms and minimize intrinsic mechanisms.

On the nanoscale the dominating intrinsic dissipation mechanism, determined by the material properties, can be explored at low temperatures. From the low temperature response of single crystal silicon resonators at both kilohertz [7] and megahertz [8] frequencies, it is clear that low-lying excitations of internal defects or two-level systems (TLS) provide the dominant contribution to intrinsic dissipation. Even though the general trend of the low temperature dependence is easily explained by the standard glass model of TLS [9, 10], additional experiments in other materials such as GaAs [11] and detailed theoretical calculations [12] suggest a lack of full understanding of the temperature dependence of the quality factor. Here, we report a detailed set of low temperature measurements in a novel material, ultra-nano-crystalline diamond (UNCD). We find that resonance frequency shift and quality factor of resonators fabricated from UNCD, single-crystal silicon, and epitaxially-grown GaAs show universality in their temperature dependence. The universal behavior provides further evidence that intrinsic dissipation in nanomechanical resonators are dominated by surface effects, whether they are (substitutional) crystal impurities or (configurational) surface defects caused by the abrupt lattice termination. Our measurements indicate that the same TLS processes dominate in a range of materials, underlining the need for a single material independent theory.

In particular, polycrystalline diamond is an exciting material for nanomechanical devices due to its unique combination of physical and electrical properties. NCD (nanocrystalline diamond) exhibits similar properties to bulk diamond, including extremely high Young's modulus and remarkable thermal conductivity. This enables high normal-mode frequencies in nanomechanical resonators, compared to silicon devices of similar sizes, that can cool efficiently down to millikelvin temperatures. The UNCD used here is distinguished by its ability to be grown so that a low surface roughness is maintained over a large range of thicknesses. Electrical properties can be varied over a wide scale by controlling the doping concentration. Here low doped wafers are used and the material is assumed to be highly insulating.

We find that dissipation follows a power law in temperature, $Q^{-1} \propto T^{\frac{1}{3}}$, independent of resonance frequency and material. At low temperatures, below 100 mK, dissipation saturates. Upon cooling, a shift in the sound velocity $\delta v/v_0$ can be observed. This is equivalent to measuring the frequency shift $\delta f/f_0$. Below a characteristic temperature $T_c \approx$ 1-2 K, where resonant absorption processes of TLS are active, we observe a logarithmic temperature dependence with a positive slope. Above T_c, TLS relaxation-absorption mechanisms dominate. The temperature dependence is also logarithmic, however with a negative and steeper slope. Interestingly, the slope of $\log(\delta f/f_0)$ scales with f_0^{-1}. We find that data from sub-micron-sized mechanical resonators from UNCD, single crystal silicon and GaAs heterostructures can be scaled onto a universal curve for both $\delta f/f_0$ and Q^{-1}.

The nanomechanical resonators (Fig. 1 a) are fabricated using standard micro-machining procedures (e-

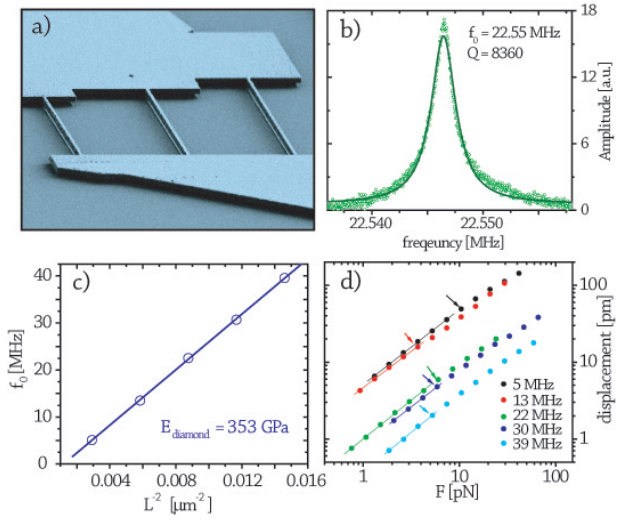

FIG. 1: (color online) a) SEM micrograph of the diamond harp structure with three doubly clamped beams. Each beam is 350 nm wide, 340 nm thick, and varying lengths of 8.3, 9.3 and 10.7 μm, two additional beams with lengths 13.1 and 18.5 μm are also included in the measurements. b) 22.5 MHz resonance with lorentzian fit of 10.7 μm doubly clamped beam. The quality factor of 8360 is measured at 35 mK and with a 6 T field. c) Frequency-length relation including a linear fit from which the Young's modulus of 353 GPa is determined. d) Plot of displacement vs. force for all five fundamental resonances, from the inverse of the slope the effective spring constant of order unity is measured. The arrows mark the onset of non-linearity.

beam lithography, metalization, reactive ion etching and finally an HF wet-etch to release the structures). The samples are etched from 340-nm thick Aqua25 films obtained from Advanced Diamond Industries, INC. Mechanical resonances from five doubly-clamped beam structures of 350 nm width and lengths varying from 8.3-18.5 μm are studied. The structures are actuated and detected by the magnetomotive technique [13] in high vacuum. Resonance frequencies f_0 and dissipation $Q^{-1} = \Delta f/f_0$ are obtained from a lorentzian fit (illustrated for the 22 MHz resonance in Fig. 1 b).

The length dependence of frequency is depicted for the five structures in Fig. 1 c). Inclusion of the effect of the metallic electrodes on top of the diamond modifies the resonance frequency: $f_0 = \eta\sqrt{(E_d I_d + E_m I_m)/(\rho_d A_d + \rho_m A_m)}L^{-2}$ [Ref.[14]]. The precise fit validates the use of the thin-beam approximation. From the slope, we determine the Young's modulus of the thin film to be 353 GPa. This is considerably lower than expected, when compared to the Young's modulus previously measured in polycrystalline diamond [15]. The Raman spectrum of the film indicates a strong presence of sp^3 bonds, however it is common that thin film diamond contains a large number of sp^2 bonds on grain boundaries, which degrade the Young's modulus. UNCD is particularly sensitive to this as the high density of nano-crystal grains effectively increase the surface area were the sp^2 bonds form. Compressive strain originating from the higher expansion coefficient of the underlying silicon that supports the diamond beams may further lower the resonance frequency, and therefore, reduce the observed Young's modulus. Fig. 1 d) shows the displacement on resonance, $x(f_0) = F_{dr}/k_{eff}$ as a function of the drive force, $F_{dr} = BLV_{dr}/R$, for all five beam resonances, where the measured magnetomotive response, $V_{emf}(\omega_0) = \frac{\xi L^2 B^2 Q}{m\omega_0} I_{dr}(\omega_0)$, is proportional to the beam amplitude [13]. The effective spring constant k_{eff} is determined from the inverse of the slope and found to be on order unity for all structures. For the remaining data, care is taken to drive the resonators only in the linear regime.

There are a number of dissipation mechanisms that are known to contribute to loss in nanomechanical resonators. By measuring dissipation as a function of frequency and temperature, one can identify the dominant contributions. Figure 2 a) depicts the temperature dependence for three resonance frequencies; the insert illustrates how dissipation varies with frequency at two applied magnetic field strengths. Short, doubly-clamped beams often suffer from clamping losses where dissipation is dominated by energy loss into the pads [15]. In this case, dissipation rapidly grows with decreasing resonator length. We observe the opposite behavior, and hence, we can rule out clamping loss as a dominant dissipation mechanism. Thermoelastic damping decreases with frequency; this mechanism however has been shown not to contribute at low temperatures and small structure sizes [16]. Internal losses in the electrode also contribute to dissipation: $Q^{-1} = 1/(1+\beta)(Q_d^{-1} + \beta Q_{Au}^{-1})$ with $\beta = (E_{Au}t_{Au})/(E_d t_d) = 0.02$. A conservative estimate for losses in the gold electrode predicts an effect smaller than ($< 5\%$). It can be shown that magnetomotive damping is proportional to $f_0^{-1.5}$. The insert of Fig. 2 a) shows good agreement with this prediction for applied fields of 6 T and 3 T. At high frequencies, magnetomotive damping no longer contributes as indicated through a saturation of the data. For the remainder of the dissipation data discussed in this letter, measurements are taken at 3 T, in the regime where magnetomotive damping can be neglected. For the frequency shift data, the measurements are taken at 6 T, as no significant field dependence of this variable is observed.

The presence of TLS becomes apparent through the temperature dependence of both dissipation, and, in particular, resonance frequency, displayed in Fig. 2 a) and b) respectively. Dissipation saturates below 100 mK with a possible recurrence beginning at temperatures above 2-4 K, observable for the lowest frequency. Within this temperature range, dissipation follows a power law, $Q^{-1} \propto T^{\alpha}$ with $\alpha \approx 0.35$, with no observed frequency correlation. At higher field strengths, where magnetomo-

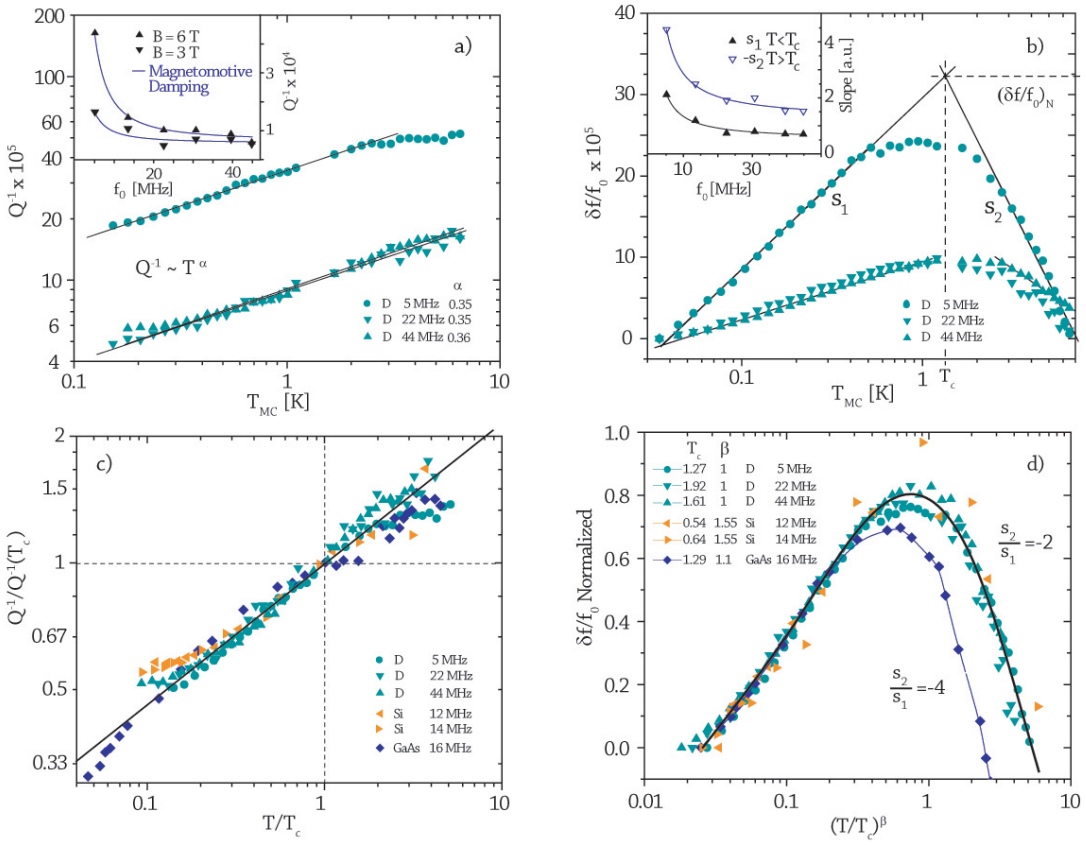

FIG. 2: (color online) a) Dissipation dependency on temperature for three resonance frequencies at 3 T. We measure $Q^{-1} \propto T^{\alpha}$, where $\alpha \approx \frac{1}{3}$. Below 100 mK the dissipation saturates. Insert: Dissipation-frequency relation at 6 T and 3 T, including fits for magnetomotive damping ($Q^{-1}_{MMD} \propto f_0^{-1.5}$). b) Frequency shift $\delta f/f_0$ dependency on temperature, where f_0 is the resonance frequency at 35 mK, measured at 6 T. Below and above a characteristic temperature T_c the shift is logarithmic as predicted by TLS models. The insert depicts the slopes of $\delta f/f_0$ for low (s_1 solid black triangles) and high (s_2 empty blue triangles) temperature regimes. The fit shows a f_0^{-1} behavior. c) Normalized dissipation $Q^{-1}/Q^{-1}_{T_c}$ for UNCD (cyan), Si [8] (orange) and GaAs [11] (blue) for frequencies ranging from 5 MHz to 44 MHz. The temperature has been scaled to T_c (see panel b)). The black solid line represents a slope of $\frac{1}{3}$, alluding to the same power law for all three materials. d) Scaled frequency shift vs. $(T/T_c)^{\beta}$. $\delta f/f_0$ has been normalized to $(\delta f/f_0)_N$ (see panel b)). All three materials behave qualitatively equivalently. The curves collapse if the ratio s_2/s_1 is constant, β is chosen as a free material-dependent parameter. The black curve is a guide to the eye.

tive damping and possibly magnetic field-TLS coupling occurs, the temperature dependence becomes weaker, while the decreasing trend is steeper for lower frequencies (data not shown).

The lack of a clear frequency dependence of α measured at 3 T indicates that the measurements were taken in the parameter space where field coupling can be neglected. The frequency shifts vs. temperature plots show a logarithmic dependence, whereas at T_c the slope changes sign and increases in magnitude. The logarithmic behavior is in good agreement with glassy TLS models, however the slope is expected to remain constant in magnitude above T_c (Phillips model [10]). The fit results are summarized in table I. We observe that the magnitude of the slope s_i doubles for $T > T_c$ independent of frequency, where s_1 is the slope for $T < T_c$ and s_2 is the slope for $T > T_c$. The slopes show an inverse dependence on frequency, also not predicted by standard theories. However this behavior has been observed by Kleiman et al. [7] in previous work on single crystal silicon resonators as well. T_c shows a rising trend with increasing resonance frequency. A precise dependence, however, could not be determined from the available data.

At low temperatures, TLS are reduced to a nearly degenerate ground state, modeled by an asymmetric double well potential with asymmetry Δ and tunnel splitting energies Δ_0, typically on the order of 1 K. Glassy models generally assume a constant density of states, independent of Δ and Δ_0, given by $P(\Delta, \Delta_0)d\Delta d\Delta_0 = \frac{P_0}{\Delta_0} d\Delta d\Delta_0$. The Phillips TLS model assumes a more constrained model with a fixed splitting energy and a gaussian asymmetry distribution with width Δ_1, while the density of states takes the form $P(\Delta)d\Delta = A \exp(-\Delta^2/2\Delta_1^2)d\Delta$. For both models the

TABLE I: Fit results for the temperature dependency on $\delta f/f_0$ for both temperature regimes ($T < T_c$ s_1, $T > T_c$ s_2). The diamond and silicon resonators show roughly similar slope ratios $-s_2/s_1 \approx 2$, while for GaAs the magnitude of this ratio significantly greater $-s_2/s_1 \approx 4$. The s_2 values quoted for silicon are rough estimates, as not enough data is available for high confidence. T_c is defined as illustrated in Fig. 2 b).

Material	f_0 [MHz]	s_1 $\times 10^{-5}$	s_2 $\times 10^{-5}$	$-\frac{s_2}{s_1}$	T_c [K]
UNCD	5.11	21.2	-44.3	2.09	1.27
UNCD	13.50	12.0	-24.8	2.07	1.86
UNCD	22.55	7.5	-19.0	2.53	1.61
UNCD	30.71	8.0	-19.9	2.48	1.91
UNCD	39.59	7.2	-15.3	2.12	1.71
UNCD	44.85	7.1	-15.1	2.11	1.92
Si	12.03	1.8	(-4.6)	(2.59)	0.54
Si	14.59	2.0	(-3.1)	(1.59)	0.64
GaAs	15.82	13.5	-55.7	4.13	1.29

logarithmic dependence of the frequency shift is reproduced, with different coefficients. Standard single crystal models predict non-logarithmic temperature dependence of the frequency shift and non-power-law temperature dependence of the dissipation, in contrast to what we observe in the data. These theoretical results are summarized in [8]. Considering the large surface to volume ratio of UNCD one expects a high density of TLS's. Theories have been developed to take interacting TLS's into account [9], these too however fail to expiation the observed behavior. In Fig. 2 c) and d), for comparison we also include previously-published data on silicon and GaAs resonators in the same temperature range.

Interestingly, the temperature dependence for both frequency shift and dissipation scales to a universal curve for all the three materials studied in this range of temperature. For scaling, the measured temperature is referenced to the characteristic temperature T_c defined in Fig. 2 b). All dissipation plots are normalized to the dissipation value measured at T_c, $Q^{-1}/Q^{-1}_{T_c}$ and plotted vs. T/T_c. Fig. 2 c) illustrates the power law $Q^{-1} \propto T^{\frac{1}{3}}$ for the three materials. Low temperature saturation is observed in diamond as well as in silicon. This is not however seen in the GaAs resonator. To compare the shift in frequency for different temperatures, the data is normalized to the values for $(\delta f/f_0)_N$, defined in Fig. 2 b) and plotted vs. $(T/T_c)^\beta$, here β is a free scaling parameter. Although there are not enough temperature data points for the silicon resonators, it appears that the three materials behave similarly in that above T_c the slope of $\delta f/f_0$ not only changes sign but also increases in magnitude (see Fig. 2 d)). Similar observations have been made in very different structures as well [14].

It is believed that the large surface to volume ratio belie the presence of a crystal, resulting that the NEMS behave like glassy structures. The data appears to fall into universality classes defined by the s_2/s_1 ratio. The scaling parameter β can be chosen as a constant for a given material, this must still be confirmed with future experiments. The universal behavior of these NEMS devices motivate the search for a theory that captures more accurately the observed relations. It is still to be seen if it is possible to reproduce theoretically the dissipation law by tuning the density of states for the TLSs.

In conclusion we report the presence of TLSs in UNCD diamond resonators at megahertz frequencies. Both the resonant absorption and relaxation absorption regimes are included with a characteristic temperature around 1-2 K. A constant power law in dissipation and analogous logarithmic frequency dependence on temperature is found and compared to measurements in silicon and GaAs NEMS resonators. Further development of the theories are required to fully explain this universal behavior, possibly taking more involved TLS density of states into account.

We thank Guiti Zolfagharkhani et al. and Seung Bo Shim et al. for making their data available to us. We thank Antonio Castro Neto and Eduardo Lopez for helpful discussions. This work is supported by the National Science Foundation (DMR-0449670).

[1] I. Martin and W. H. Zurek, Phys. Rev. Lett. **98**, 120401 (2007).
[2] M. Bocko and R. Onofrio, Rev. Mod. Phys. **68**, 755 (1996).
[3] H. J. Mamin and D. Rugar, Appl. Phys. Lett. **79**, 3358 (2001).
[4] D. Rugar, R. Budakian, H. J. Mamin, and B. W. Chui, Nature **430**, 329 (2004).
[5] C. Montemagno and G. Bachand, Nanotech. **10**, 225 (1999).
[6] G. Wu, H. Ji, K. Hansen, T. Thundat, R. Datar, R. Cote, M. Hagan, A. K. Chakraborty, and A. Majumdar, Trans. Nat. Acad. Sci. U.S.A. **98**, 1560 (2001).
[7] R. N. Kleiman, G. Agnolet, and D. J. Bishop, Phys. Rev. Lett. **59** (18), 2079 (1987).
[8] G. Zolfagharkhani et al., Phys. Rev. B **72**, 224101 (2005).
[9] P. Esquinazi, ed., *Tunneling Systems in Amorphous and Crystalline Solids* (Springer (Berlin), 1998)
[10] W. A. Phillips, Rep. Prog. Phys. **50**, 1657 (1987).
[11] S. B. Shim et al., Appl. Phys. Lett. **91** (13), 133505 (2007).
[12] C. Seoanez, F. Guinea, and A. H. Castro Neto, EPL **78**, 60002 (2007).
[13] P. Mohanty et al., Phys. Rev. B **66**, 085416 (2002).
[14] Y. T. Yang et al., Appl. Phys. Lett. **78**, 162 (2001).
[15] M. Imboden et al., Appl. Phys. Lett. **90**, 173502 (2007).
[16] T.V.Roszhart, Solid-State Sensor and Actuator Workshop, 1990. 4th Technical Digest., IEEE, **13**, (1990).